
Article:
Quintana-Nedelcos, A., Anis, M., Osman, R. et al. (4 more authors) (2022) On the structural, microstructural and magnetic properties evolution of Ni0.5FeCoAlCrx alloys. Materials Letters, 311. 131542. ISSN 0167-577X

https://doi.org/10.1016/j.matlet.2021.131542

On the structural, microstructural and magnetic properties evolution of $Ni_{0.5}FeCoAlCr_x$ alloys.

A. Quintana-Nedelcos[1,2,a], M. Anis[1], R. Osman[1], J. Yang[1], Z. Leong[1], Y. Azakli[1] and N. A. Morley[1,b]

[1]Department of Materials Science and Engineering, University of Sheffield, Sheffield, S1 3JD, UK

[2]New Model Institute for Technology and Engineering, Blackfriars St., Hereford HR4 9HS, UK,

[a] aris.quintana-nedelcos@nmite.ac.uk, [b] n.a.morley@sheffield.ac.uk

Abstract

The multicomponent alloy CoFeNiAlCr has shown great promise as a soft magnetic material due to its small coercive field and high saturation magnetisation at room temperature. By changing the ratio of the components, the Curie temperature can be tuned, along with improvements in both the coercive field and saturation magnetisation. The alloy system is interesting as the ratio of Al to Cr determines whether a single solid phase or a dual phase alloy is formed. This work has investigated the effects of Cr addition on the structural and magnetic properties of $CoFeNi_{0.5}AlCr_x$. It discusses the evolution of the NPs-matrix segregations and its constituents' phases.

Keywords

CoFeNiAlCr; Magnetic properties; High Entropy Alloys; Multicomponent Alloys; Phase Segregation; Nano-Particles;

Introduction

Multicomponent alloys, commonly known as High-entropy alloys (HEAs) are of high interest for both fundamental and applied research due to the unique combination of properties that they exhibit. The majority of research has focused on their mechanical properties, but there is an increasing interest in understanding their magnetic properties [1,2,3]. These have been found to be highly dependent on their phase evolution and/or phase separation [4,5,6,7].

Previously, we have investigated the $CoFeNi_{0.5}Cr_{0.5}Al_x$ (x = 0.0, 0.5, 1.0 and 1.5) alloy system to evaluate its potential use in high temperature magnetic cooling and energy harvesting technologies [8], by studying its magnetic entropy change (ΔS_m). These prove to be competitive if compared to others second order phase transitions (SOPT) materials with Curie temperatures (Tc) above room temperature, but still lower to those showing a first order phase transition (FOPT). However, regardless of the relatively low ΔS_m values, the analysis proved to be a useful tool to further comprehend phase contribution to the magnetic properties. Further, we reported that the FeCr nano-particles (NPs) phase segregation within AlNiCo rich matrix [8,9], was driven by the Al addition, which was concomitant to a FCC ($CoFeNi_{0.5}Cr_{0.5}$) to BCC/B2 ($CoFeNi_{0.5}Cr_{0.5}Al_x$, x = 1.0 and 1.5) phase evolution. For the fully segregated NPs-matrix samples, we found two distinctive transition regions (High Temperature Transition (HTT) and Low Temperature Transition (LTT)), with their own characteristic T_C,. FeCr-NPs were found to have the highest magnetization. However, their contribution to the total magnetization was determined by the interaction among them, being highly sensitive to their size and the matrix-LTT transition [8].

In the present contribution we studied and analysed the role of Cr in this HEA family ($CoFeNi_{0.5}AlCr_x$; x = 0.25, 0.50, 0.75 and 1.00).

Experimental

Synthesis: Samples of the stoichiometric composition of $CoFeNi_{0.5}AlCr_x$ ($CFNACr_x$, x = 0.25, 0.50, 0.75 and 1.00) were arc-melted at least three times in an Edmund Buhler Compact Arc Melter (components >99% purity). The samples were heat treated at 1423 K for 10 hours in Argon atmosphere before being air cooled. Thereafter samples will be named as Cr025, Cr050, Cr075 and Cr1.

The pair analysis was performed by considering the binary enthalpies of mixing calculated from Miedema's method of the compositional alloying additions. For 5-components, 10 pairs are evaluated according to a Monte-Carlo scheme consisting of an atomic population (>1,000 atoms) that matches the compositional stoichiometry. The probability of a pair being picked is evaluated by evaluating a modified Arrhenius relationship where the energy term is substituted with each binary enthalpy of mixing value.

Characterisation: A Hitachi TM3030 Plus microscope was used for scanning electron microscope (SEM) imaging. X-ray diffraction (XRD) using a Bruker D2 phaser. A Quantum Design MPMS-3 system was used to determine the magnetic properties. Field-cooling (FC) and field-heating (FH) thermomagnetic $M(T)$ curves were measured for applied static magnetic fields ($\mu_0 H$) of up to 2.0 T at a heating/cooling rate of 5 K/min. Curie temperatures were determined from the peak in the $\delta M(T)/\delta T$ plots. $\Delta S_m(T)$ curves were obtained from a set of magnetisation isotherms, $M(H)$-virgin loops, the standard thermal protocol was used.

Discussion and analysis.

Analysis: Structural and microstructural analysis.

XRD data (Figure 1(a)) determined that the main phase present in all the samples was a BCC/B2 type with a dominant (110) peak, in agreement with previous results [9]. A pair analysis of the enthalpy of mixing values was used to estimate the most likely binary alloys that would form together, along with the expected percentage of occurrence for each $CFNACr_x$ alloy, Figure 1(b). The CoAl and NiAl pairs have the highest expected percentage of occurrence, followed by the CoCr pair.

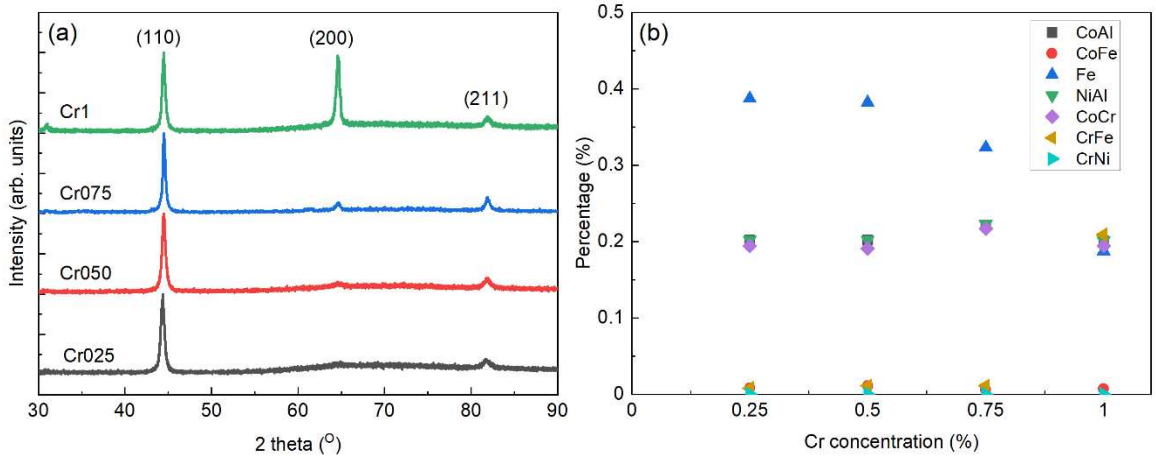

Figure 1. XRD (a) and the expected percentage occurrence of the possible binary alloys (a) for $CoFeNi_{0.5}AlCr_x$ alloys.

For a better understanding of the functionalization of the alloy with Cr content and therefore the magnetic properties, the evolution of the Fe element and its pairing products are important. Notice that Fe shows an evolution from a highly unpaired percentage (Cr025) to an increased pairing percentage occurrence for further Cr addition. The change is concomitant to the observation of the formation of FeCr and FeCo pairs where the suggested driving mechanism is their similar crystal

structure [10]. In turn, new pairing expectancy in the $CFNACr_x$ samples show a strong dependency to the Cr content. Thus, CoFe, NiAl, CoAl and CoCr pairs expected occurrence percentage remains across all $CFNACr_x$ samples. While the occurrence of CrFe pairing increases with Cr content increase, so decreasing the unpaired Fe percentage. This aligns to the previous description of the FeCr-rich NPs segregation into an AlNiCo-rich matrix for similar systems [5,8,9], which distinctive features can be observed in the SEM micrographs taken of the $CoFeNi_{0.5}AlCr_x$ surfaces (Figure 2).

Building on the FeCr-rich NPs + AlNiCo-rich matrix description but taking account of the different pairs expected occurrence evolution, we can hypothesise that Fe-rich sites act as the nucleation (core) sites for the NPs to form while its interface with the AlNiCo-rich matrix is formed by a FeCrCo (CrFe+CoFe) rich area (shell). For instance, we can envisage that the nucleation and growth of NPs is predicted to happen with as little as Cr025 addition. Experimentally, if this happened, it was at a scale that the SEM could not resolve (Figure 2). With further Cr addition (Cr050 and Cr075), fewer Fe-core occur, which is balanced with an increase in CrFe pairing, thud a decrease in the number of NPs, but these will be larger in size. These features can now be seen in the SEM images as light-grey precipitates and the phase partially wetting the AlNiCo-rich grains [11] (Figure 2). For further increase (Cr1) this will lead to large FeCr-rich precipitates and continuous phase in the grain boundaries that compete in extent with the AlNiCo-rich matrix (Figure 2), including micron size rectangular grains of similar composition to the NPs. As result of this, the two main phases (FeCr-rich and AlNiCo-rich phases) are now similar in their overall display.

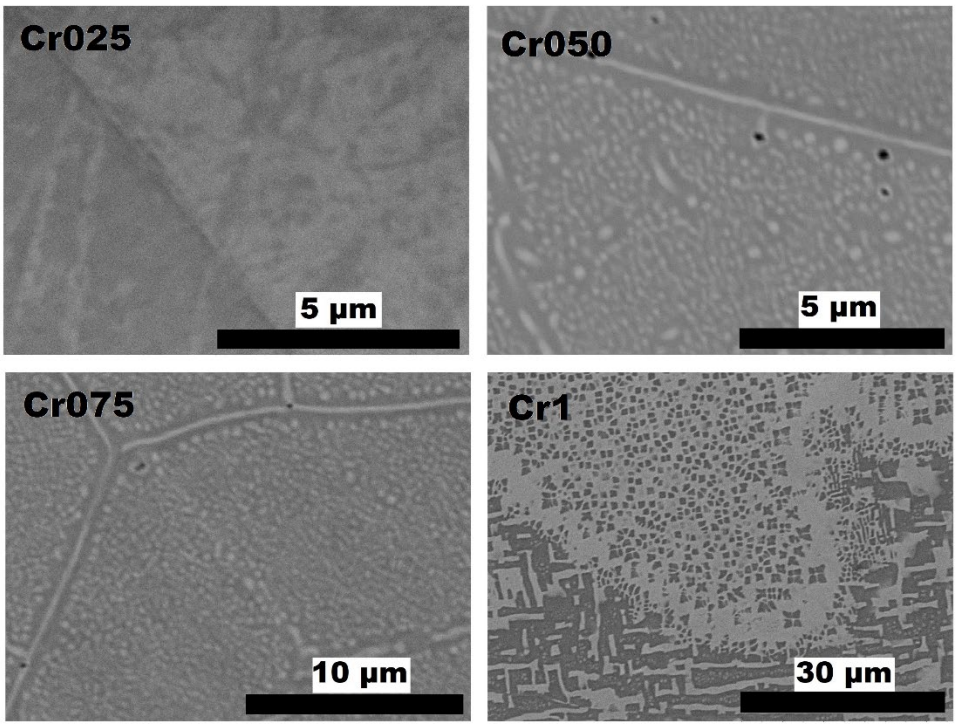

Figure 2. SEM images of $CoFeNi_{0.5}AlCr_x$ alloys.

Analysis: Magnetic properties.

In the preceding section we theorised on the formation of a core-shell structure as a better description to what was previously described FeCr-rich NPs [5,8,9]. This couldn't be resolved with structural and/or microstructural analysis, so the following magnetic analysis provides further support.

Figure 3 shows ΔS_m measured from 1000 K to 500 K for the $CoFeNi_{0.5}AlCr_x$ samples. Notice that the curves reveal the same two temperature regions: LTT and HTT where, LTT < 850 K and HTT > 850 K, from the previous study of $CoFeNi_{0.5}Cr_{0.5}$-Al_x system where they are linked to the matrix and NPs regions respectively [8,9]. Within the HTT region there are at least two peaks, the main peak, identified as the one with the highest value of ΔS_m and secondary peaks or shoulders that appear to the right of the main peak. Similar behaviour was observed in [8] where it was argued that this is due to the FeCr-NPs domain walls being pinned to other phases while in their crystallization process. Ultimately leading to a core-shell structure of the NPs determined by the interactions of its constituents with the matrix at the NP-matrix interface.

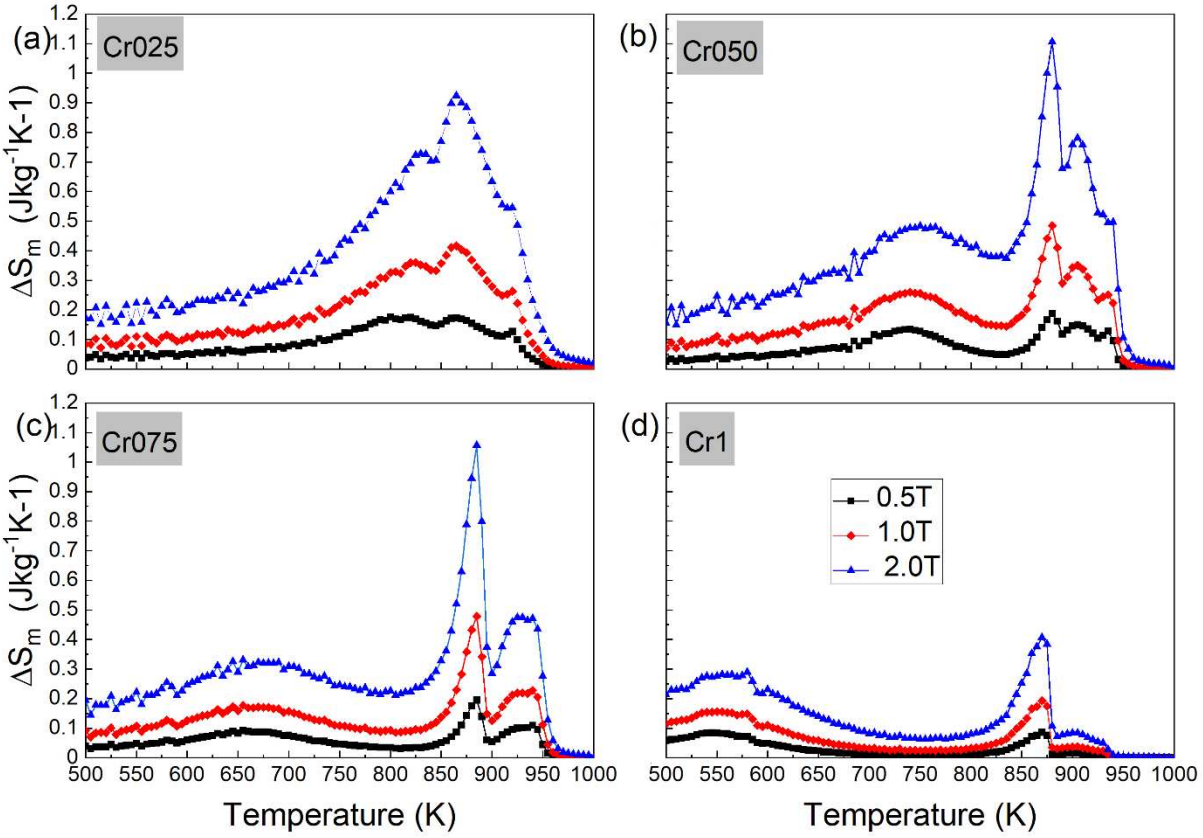

Figure 3 Magnetic entropy change (ΔS_m) for samples Cr025 (a), Cr050(b), Cr075(c), Cr1(d).

For the HTT region, the peak configurations (main peak + shoulders) seem to be independent (position wise) of the Cr content. However, the relatively height of the main peak regarding its shoulder increases with Cr addition, suggesting that the main peak can be linked to the FeCr pair and the shoulders to the Fe + FeCo constituents in the core-shell structure.

For the LTT region T_{peak}^{LTT} decreases with the increase in Cr. The Cr025 sample has the highest $\Delta S_{m,peak}^{LTT}$ at 830 K, which is close to the $\Delta S_{m,peak}^{HTT}$ at 865 K, suggesting the phases have not fully develop yet from one another (as observed in the SEM image). As more Cr is added, this will pair with both Fe and Co (figure 1(b)) affecting both NPs and matrix composition, structure, microstructure and magnetic properties. For instance, as the Cr content in the matrix increases, T_C^{LTT} decreases due to its antiferromagnetic alignment with the rest of the elements (Ni, Co) [6]. While T_{peak}^{HTT} remain similar as the Cr/Fe ratio remains constant around the equilibrium ratio. This interpretation is consistent with the $\delta M(T)/\delta T$ data presented in Figure 4.

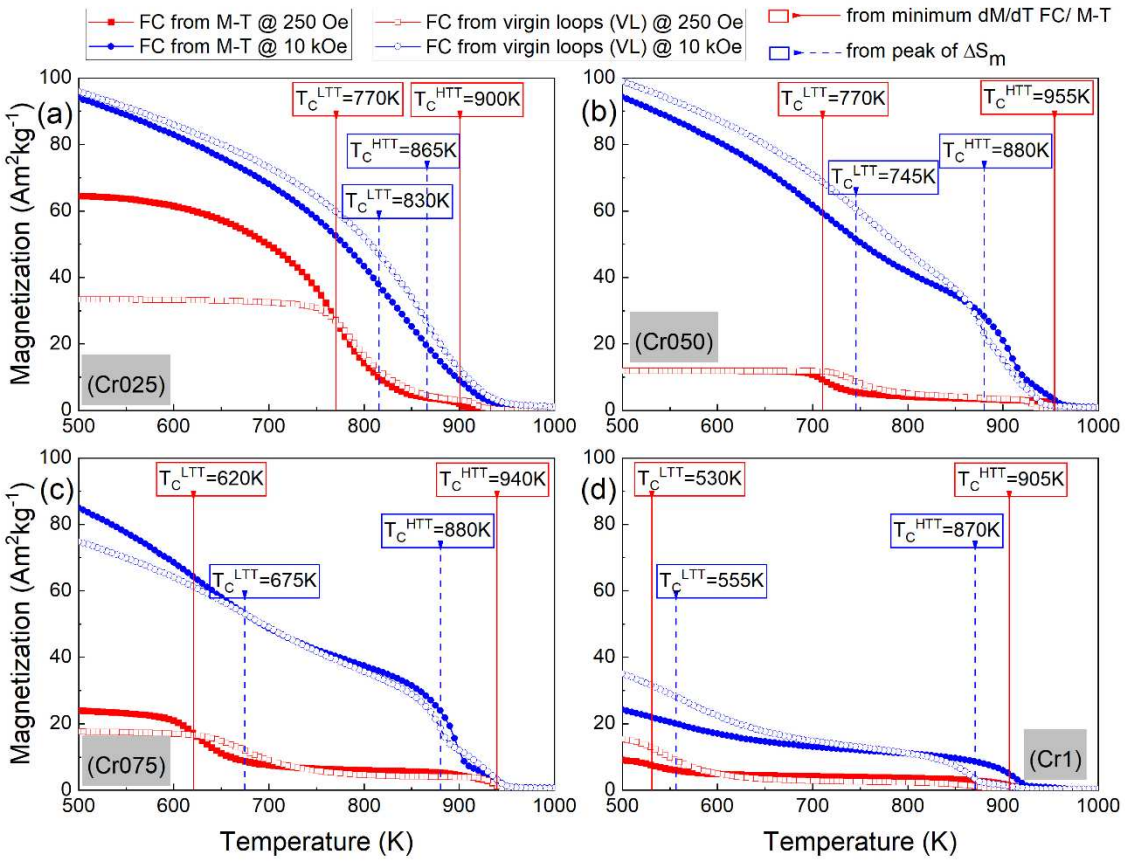

Figure 4 FC path of direct *M(T)* measurements curves (solid symbols) and the indirect magnetisation dependence on temperature (MT) curve obtained from isothermal measurements of VL (open symbols) at applied fields of 25 mT (blue) and 1.0 T (red). Solid vertical red lines indicate the T_C^{LTT} and T_C^{HTT} as measured from the minimum of the derivative ($\delta M(T)/\delta T$) of the FC path. Dashed vertical blue lines indicate the T_C^{LTT} and T_C^{HTT} transition temperatures as measured from ΔS_m^{peak}.

Moreover, variances in the path of the isofield and isotherm *M(T)* curves show the different effects on the magneto-thermal history of the material when subject to a field or thermal induced reversal. Hence, the complex interaction between the NPs, and NPs-matrix, which we believe that for a greater understanding of it future studies should focus on understanding the core-shell structure of these NPs.

Conclusions

We have investigated the evolution of the structural, microstructural and magnetic properties of the $Ni_{0.5}FeCoAl$-Cr_x alloy family. We found that Cr pairing occurrence with Fe drives the formation of a core-shell structure of the segregated NPs. Being this nucleated around unpaired Fe elements. With Cr addition there are more FeCr formed, with less Fe leftover, leading to fewer but larger NPs. Added Cr keeps T_C^{HTT} unchanged around an optimum/equilibrium Fe/Cr ratio while T_C^{LTT} will decrease due to excess Cr going to the matrix. It was shown the fundamental role of Cr to determine the structural and magnetic properties of this materials magnetic functionalization by driving its dual phase functionalisation.

Contributions

Experimental design (A.Q.N., N.A.M.), Formal analysis (A.Q.N, N.A.M, Z.Y.L.) Writing (A.Q.N, N.A.M.) Conceptualization (A.Q.N., N.A.M.), Methodology (A.Q.N., N.A.M., Z.Y.L), Investigation (A.Q.N, N.A.M., Z.Y.L, M.A., R.O., Y.A., J.Y.), Funding acquisition (N.A.M.).

Acknowledgements

Work supported by Leverhulme Trust Fellowship (SRF\R1\180020) and (RPG-2018-324)

References

[1] V. Chaudhary et al, *Mater. Today*, vol. 49, pp. 231-252, 2021.

[2] J. Y. Law et al, *APL Mater.*, vol. 9, p. 080702, 2021.

[3] R. Kulkarni et al, *J. Alloys Compd.*, vol. 746, pp. 194–199, 2018.

[4] Y. Ma *et al.*, *Metals (Basel).*, vol. 7, p. 57, 2017.

[5] W. R. Wang et al, *J. Alloys Compd.*, vol. 589, pp. 143–152, 2014.

[6] T. Borkar *et al.*, *Adv. Eng. Mater.*, vol. 19, no. 8, p. 1700048, 2017.

[7] K. Baba et al, *Materials (Basel).*, vol. 14, p. 2877, 2021.

[8] A. Quintana-Nedelcos et al, *Mater. Today Energy*, vol. 20, p. 100621, 2021.

[9] N. A. Morley et al, *Sci. Rep.*, vol. 10, p. 14506, 2020.

[10] Y. Duan et al, *J. Magn. Magn. Mater.*, vol. 497, p. 165947, 2020.

[11] B. B. Straumal et al, *J. Mater. Eng. Perform., vol. 21 pp. 721-724, 2012.*